





Procedurally Generated Age-related Visual Deficits in Virtual Reality Environments

C. Zavlanou^{1,2} , P. Huber³, Y. Tisserand² , D. Rudrauf² , A. Lanitis^{1,4} 

¹Visual Media Computing Lab, Cyprus University of Technology, Cyprus

²The Laboratory of Multimodal Modelling of Emotion and Feeling, University of Geneva, Switzerland

³Division of Internal Medicine for the Aged, University Hospitals of Geneva, Switzerland

⁴CYENS Centre of Excellence, Cyprus

Abstract

The simulation of visual deficits associated with aging has been the subject of numerous investigations both in real environments with the use of aging suits and in immersive environments with the use of Extended Reality experiences. However, there is a dearth of heterogeneity and randomness, which characterize the age-related conditions and are important aspects in human-like simulations. Towards this end, procedurally generated age-related deficits are simulated in Virtual Reality environments, giving the possibility to experience these deficits and their nuances in real time. Our work is drawing upon state-of-the-art feature-based approaches, such as foveated rendering and procedural noise, to provide realistic effects. A pilot assessment is conducted through a visual performance task, while eye-tracking data are recorded. The preliminary results provide a first evaluation of the simulation's effectiveness in inducing, in normal subjects, a visual behavior similar to that of real patients.

CCS Concepts

• **Computing methodologies** → Compute shaders, foveated rendering, procedural noise; • **Hardware** → Virtual Reality, eye-tracking;

1. Introduction

Perspective-taking is recognized as being an effective means of understanding another individual's condition. Among other fields, this principle has been used to allow healthcare professionals, designers, and other stakeholders, to better understand the physical challenges faced by many elderly people. For this, various approaches have been employed, from conceptual ones such as the use of elderly personas in user-centered design, to practical ones, such as the simulation of physical challenges using special apparatus. The latter has a long-standing history and has been the subject of numerous investigations in real-life settings and virtual environments (VE), alone or in combination.

In real environments, a typical form of aging simulation is the aging suits [LDG*17], a method used in specific cases, such as in the medical education [HSSG12]. It has been used to give a hands-on experience of what is like to live as an elderly person with specific age-related deficits. The advantage offered by aging suits is that they provide an integrated solution to simulating several physical age-related declines, from visual impairment to decreased mobility. In virtual and semi-virtual environments, the existing approaches have principally targeted visual deficits, leveraging the advance of Extended Reality (XR) technologies.

Computer-generated simulations nowadays are far ahead, in terms of quality and realism of the static effects offered by the aging suits,

in that they include important features, such as gaze-contingent, and dynamic effects that can be adjusted in real time.

The aim of this research is to integrate heterogeneous, age-related visual deficits in VEs through a novel approach based on procedurally generated effects, to increase the realism of the latter by incorporating the aspect of randomness.

In collaboration with a geriatrician, we focused on three specific classes exhibited in two common deficits, namely metamorphopsia and macular scotomas in Age-related Macular Degeneration (AMD), and peripheral visual field loss following glaucomatous damage. The deficits were simulated in a VE setting, using dedicated compute shaders compositing procedural noise.

During the development process, an external review was conducted by three ophthalmologists based on rendered videos of the VR-based simulation. Following their feedback, several improvements of the simulated effects were reconsidered.

2. Background and Related Work

An early elaborate effort towards computerized simulation of eye deficits was reported 20 years ago, when a dark spot was printed on an acetate film to approximate central scotomas, animated using an eye-tracking system [FR99]. With the evolution of technology and computer graphics, this approach transformed into computer-

generated simulations [VAS08]. The quality and affordability of Extended Reality technologies further propelled the simulations of visual deficits, and numerous immersive simulations made their appearance over the last years [AGR*00] [VCH16] [JAR06]. Use cases range from universal accessibility in architecture [KBS*18] and product design [ZL18], to addressing information needs of patients and their relatives [SES18], and developing empathy in medical students [ANK*20].

In the field of Augmented Reality (AR), Ates et al. [AFF15] have transformed a VR headset into an AR system using wide-angle cameras to apply several filters on the rendering of a real environment and simulate specific eye deficits. Recently, integrating gaze-contingent effects, Krösl et al. [KEL*20] simulated cataract symptoms of adjustable severity in an AR system, evaluated by real patients.

Likewise, many VR-based approaches have been proposed. Krösl et al. [KEW*19] have developed a VR-based simulation of specific cataract symptoms, such as blurred vision, contrast, and light sensitivity. It is worth noting that this approach considers both the actual vision of the user and VR headsets' limitations to calibrate the simulation and provide a similar experience to all users.

In terms of implementation, the most typical method to simulate visual deficits in VR consists in applying post-processing effects to the images [LBCM11], [ZL18]. A more refined approach described by Stock et al. [SES18], uses actual visual field data to represent how real glaucoma modify patients' vision.

To date, the aspect of heterogeneity has mainly relied on adjusting the intensity of the effects, for example the amount of blurriness in the case of simulated cataract. There are cases in which simulations are "unique", but these correspond to the mapping of real patient data, which cannot be easily modified parametrically.

Exception to this is the work by Jones and Ometto [JO18] who follow a sophisticated method to simulate highly customized simulated effects. Unlike their approach, to generate more naturalistic simulations, we introduce the aspect of randomness in deficits that are generated procedurally in a patient-independent manner. Thus, the proposed system can generate an arbitrarily large number of simulated effects.

3. Methodology

Age-related visual deficits can be unilateral or bilateral. Bilateral cases—involving both eyes—do not necessarily imply symmetry. Instead, inter-eyes differences often appear, with one of the eyes' vision being impaired at different intensity levels [PFW*98] [Qui99]. For this reason, it is important to simulate different effects per eye and adjust the effects independently. Note that asymmetric effects are part of a module already provided in existing VR-based simulated approaches [SES18] [JO18].

Another step towards an accurate approximation of age-related visual conditions is to distinguish peripheral from central vision in the VE. This is essential, as different deficits affect different regions of the visual field (VF). For example, AMD affects principally the central vision, while glaucoma mainly affects the peripheral VF. A similar approach in which VF sectors are demarcated has recently gained currency in VR applications. Referred to as *foveated rendering*, this approach helps improving the performance in VEs, by leveraging how acuity decreases with eccentricity in the human vi-

sual system [PSK*16] [SIGK*16]. However, to our knowledge, no such approach has been applied in VR-based simulations of visual deficits.

Following the method from [SIGK*16], we calculate the radius of the region corresponding to the central vision in the VE in pixels.

$$R = \rho_{px} d_u \tan\left(\frac{\alpha}{2}\right) + c \quad (1)$$

Let d_u be the distance (in mm), between the eye and the headset's display, α the subtended visual angle of the fovea, ρ_{px} display's density in pixels/mm, and c a value accounting for tracking errors [SIGK*16]. Using Equation 1, we calculate the radius R of the circle defining the central vision in the VE. Note that the blending border of the equation from [SIGK*16] is not used, as effects' blending is considered differently in our case. Following the same process, the radii of the other sectors of the VFs are calculated. The calculations are consistent with the visual result in the VE, as according to O'Shea [O'S91], approximately two degrees of visual angle covered by central vision correspond to the width of ones' thumb with arm extended.

Similarly to other studies [JO18] [KEW*19], the simulation is synchronized with eye-tracking data to provide gaze-contingent effects. In our case, the eye-tracking module is part of a twofold approach. First, it is used to increase the naturalness of the simulated deficits and second to obtain potential patterns of visual behaviours during visual performance tasks in the VE.

A distinctive feature of our approach is the generation of noise textures that represent the affected regions of the VF. These textures are generated procedurally, based on user-defined parameters, both in near real time and offline. To achieve this, high performance GPGPU computation-based shaders are used to rapidly calculate the various mathematical equations that are required to generate the textures.

This is not the first time that image noise is used to add a naturalistic appearance to simulated human body elements. To increase realism in surgery simulations, Xuemei et al. [XHH10] showed how Perlin noise can be used to approximate the surface of specific human organs, while Jakes et al. [JBD*19] presented an approach to obtain naturalistic patterns of fibrosis using Perlin noise. Other example can be found in [DBP*15], where procedural noise was used to mimic the appearance of breast tissues to generate imaging phantoms.

3.1. Age-related Macular Degeneration

Age-related Macular Degeneration is a common disease among the elderly population [BSW*13], expected to affect 288 million people by 2040 [WSL*14]. Early AMD is a mild stage, not often characterized by particularly distinct symptoms [JMM08]. At the late stage of AMD, symptoms become prominent with visual scotomas in the central or pericentral visual field in the non-neovascular form of advanced AMD, and more severe symptoms such as sudden visual loss due to retinal hemorrhage, in the neovascular form [JMM08].

The proposed simulation focuses on common symptoms of AMD, such as the metamorphopsia, and the macular scotomas in the central and pericentral VF.

3.1.1. Central Scotomas

In AMD, spots hindering vision appear mainly at the center of the VF in the form of relative scotomas (RS) and may evolve to absolute scotomas (AS) [NFLS05]. RS do not completely block vision in affected regions, but cover it with a veil-like effect [MV16]. Instead, AS completely mask vision in the corresponding region, which patients perceive as “missing parts” [TEBC18]. To simulate central scotomas in the VE, we suppose that the effect is determined by three parameters: the *spreading* of the scotoma, its *shape*, and its *translucency*.

For the spreading, we assume that the affected area is contained within a boundary circle, concentric with the circle defining the central vision. Given that the central point of vision corresponds to the center of the mask texture, w and h refer to the width and height of the mask texture, respectively, so that the coordinates of the center of the boundary circle are $(\frac{w}{2}, \frac{h}{2})$. Thus, the dispersion of the deficit can be described through the radius of that boundary circle. Using the canonical form of a circle, we refer to its inner surface, namely the affected area, as the set of points (x, y) that satisfy the condition of Equation 2. Henceforth, when describing the central scotomas, we are referring to these set of points (x, y) .

$$(x - \frac{w}{2})^2 + (y - \frac{h}{2})^2 < r_s^2 \quad (2)$$

We assume that the center of the macular scotomas and the center of the VF coincide as this is a common form of macular scotomas. However, this does not encompass the full diversity of the real condition, as macular scotomas can also appear in other parts of central VF [MV16]. This simplification is aimed at facilitating the evaluation of the appearance of the effects, as according to [MV16], the further the scotomas appear from the center, the more complicated it is to assess their form.

Let us now define the shape and the overall appearance of the scotomas in AMD. For the most part, macular scotomas have amorphous shapes with discontinuities. To simulate these “scallop-shaped” forms [NFLS05], we apply procedural noise to make their contour and inner surface, arbitrarily undulating. The result is produced by applying Perlin noise [EMP*03]; the two coefficients, namely the frequency and the amplitude [LLC*10] can be controlled to customize the appearance of the macular scotomas.

Additionally, to simulate decreasing intensity with eccentricity, the normalized distance of each point (x, y) from the center is used in the generation of the texture. Each texture pixel (texel) represents the amount of deviation from the intact condition of the eye.

Finally, the translucency parameter controls the category of scotomas. When the variable of translucency is at zero, the simulated scotoma is considered absolute, as it completely blocks vision (Figure 1a). For values greater than zero, linear interpolation is used to blend the scotoma with the VE, producing the effect of a RS (Figure 1b).

3.1.2. Metamorphopsia

One of the first manifestations of AMD is distorted vision [TMGS94] appearing in the center of the VF. According to self-reported data, this distortion, known as metamorphopsia, is causing the image to appear “bendy”, “crooked”, “wavy”, “wobbly” or

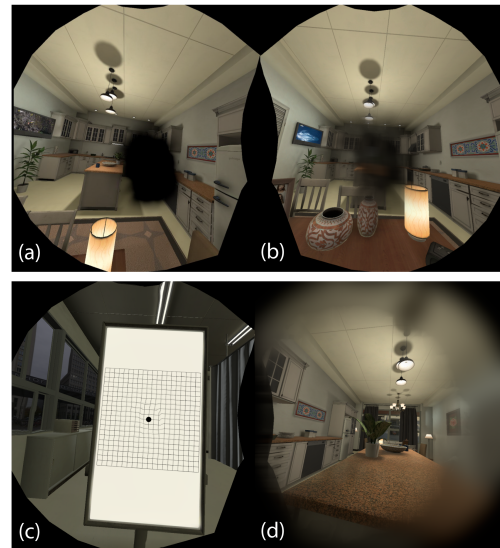


Figure 1: A simulated (a) absolute scotoma, (b) relative scotoma, (c) metamorphopsia, and (d) glaucomatous damage

“wiggled” [TEBC18]. To approximate this effect, bump textures similar to the ones described in the case of the scotomas (Section 3.1.1) are generated procedurally using Perlin noise. Each pixel value of the bump texture indicates the visual spot where the distortion occurs, and the intensity of the distortion which can be further controlled by a corresponding parameter. The distortion is achieved by shifting the UV coordinates of the image (Figure 1c).

3.1.3. Glaucoma

Glaucoma—the main cause of irreversible blindness globally [WAM14]—is a set of visual deficits [Qui99] caused by an increased intraocular pressure, which in turn damages the retinal ganglion cells (RGCs). To imitate the “death” of RGCs in the glaucomatous damage and achieve a similar result to the one obtained from visual field tests (perimetry data); Voronoi noise is used [Aur91]. Based on the nearest-neighbor rule [Aur91], the noise pattern is created as each texel gets a grayscale value according to its distance from the closest point of a set of randomly selected points (sites). In our case, the set of points considered correspond to the most affected RGCs.

The most typical symptom of glaucoma is blurred vision [HZH*14]. For this, similar to other studies [KEW*19], the resulting effect is obtained by convolving the generated texture marking the glaucomatous damage, with a Gaussian function in both dimensions (Equation 3). An additional parameter controlling the amount of blurriness allow us to obtain different intensities of blurred peripheral vision (Figure 1d).

$$G(x, y) = \frac{1}{2\pi\sigma^2} e^{-\frac{x^2+y^2}{2\sigma^2}} \quad (3)$$

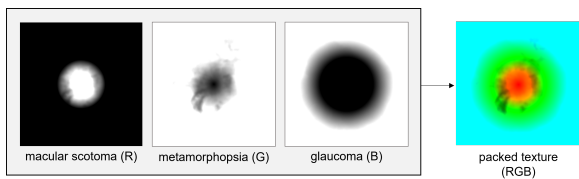


Figure 2: Example of a generated channel-packed texture containing information about a macular scotoma (red channel), metamorphopsia (green channel) and glaucomatous damage (blue channel)

3.2. Channel-packed effects

Visual deficits do not always occur in a distinct way; for example, metamorphopsia can coincide with RS [MV16]. Even the conditions per se do not always appear separately. For instance, neovascular AMD and glaucoma can coexist in the same patient [MLC*20].

For this, we added the option of packed textures to avoid generating and loading different textures for each effect. These texture masks, which can be generated both offline and at run time, encode information for each type of symptoms in a separate color channel (see Figure 2). As part of the simulation, individual channels are then extracted from the corresponding visual defect’s shader.

4. Implementation

For the implementation of the simulation, the Unity3D long-term support version (2019.4) was used, with the build-in render pipeline. For the visualization of the simulation in the VE, the HTC Vive Pro Eye headset was used with embedded eye-tracking technology by Tobii. The generation of textures detailed in Section 3 was achieved using Compute Shaders [Dop18], implementing one kernel per condition.

5. Experimental Evaluation

To investigate whether the simulation can induce, in normal subjects, virtual impairments in a similar manner to patients with actual deficits, a pilot assessment was conducted with six volunteers with normal or corrected-to-normal vision. Subjects were asked to perform a visual task, while experiencing the simulated conditions (AMD and Glaucoma) and the Normal condition, in randomized order. To enable between-subjects comparison, the same simulated effects both in the AMD and the Glaucoma condition were used for all participants. The visual performance task included the reading of a series of unrelated words based on the MNRead test [LRL*89], displayed in the VE at a viewing distance of 20 cm.

MNRead is a standardized test [LRL*89], through which significant results can be obtained about how reading rates are affected by different visual deficits [CBH*11]. In our case, the MNRead test was used, at an initial stage, to extract information about the visual behaviour that healthy subjects adopt in the VE, while experiencing the simulated effects, and compare them with the ones from real patients.

Eye-tracking data were extracted and differences in fixations between the three conditions were measured. Heat maps obtained

from the eye-tracking data are shown in Figure 3. Based on the results, fixations in the AMD condition fit the pattern of preferred retina locus (PRL), indicating that similar to real AMD patients, subjects in the VE showed a preference to fixate to a position “superior” to the scotoma [SA05] to compensate for the blind spot. Instead, as expected, fixations in the Normal condition are centrally concentrated. These initial results demonstrate that central scotomas’ simulation can produce a similar difficulty to that experienced by real patients when trying to read a text.

In glaucoma patients, fixations are mainly central [KTH*09]. However the eccentric fixation that subjects adopted during the glaucoma simulation is not surprising, as such cases may occur [KTH*09]. In any case, additional data are needed to draw more reliable conclusions.

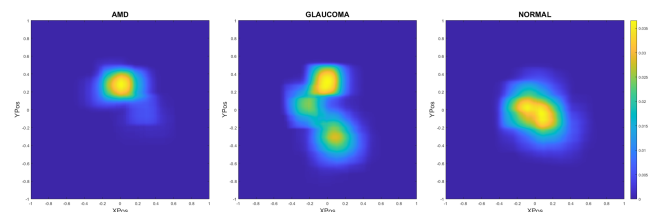


Figure 3: Eye-tracking heat maps during the AMD (left), the Glaucoma simulation (middle) and the Normal condition (right).

6. Conclusions

Much work on the potential of VR-based simulation of visual deficits has been carried out over the last years with simulations evolving from post processing effects to real data integration and use of mathematical formulas. This shows the strong interest around the approach and supports the potential of VR to yield valuable knowledge on the topic.

Our contribution lies in the addition of the aspect of heterogeneity in the simulation of specific age-related deficits in an innovative approach. Our approach focuses on the procedural generation of noise textures to simulate realistic visual deficits that can be controlled by high-level parameters. The simulation provides a diverse assortment of effects that can be generated both online and offline, allowing their use in different platforms. A pilot evaluation study was conducted in the VE with encouraging results, providing the impetus for further investigation through a larger scale testing.

Future studies could follow this approach to deal with modelling and evaluating diverse simulations of other visual impairments. Moreover, evaluation processes based on visual performance tasks could be used to investigate the effectiveness of similar simulations.

Acknowledgement

This project was partially supported by EU’s H2020 Research and Innovation Programme (Agreement No 739578) and the Government of the Republic of Cyprus.

Special thanks to Andreas Kitsis for his help in the experimental evaluation process.

References

- [AFF15] ATEs H. C., FIANNACA A., FOLMER E.: Immersive simulation of visual impairments using a wearable see-through display. In *Proceedings of the Ninth International Conference on Tangible, Embedded, and Embodied Interaction* (2015), pp. 225–228. 2
- [AGR*00] AI Z., GUPTA B. K., RASMUSSEN M., LIN Y. J., DECH F., PANKO W., SILVERSTEIN J. C.: Simulation of eye diseases in a virtual environment. In *Proceedings of the 33rd Annual Hawaii International Conference on System Sciences* (2000), IEEE, pp. 5–pp. 2
- [ANK*20] ALEXANDER D., NGUYEN T., KELLER P., ORLOSKY J., BROWN S., WOOD E., EZENWOYE O., JIRAU-ROSALY W.: Design of visual deficit simulation for integration into a geriatric physical diagnosis course. In *2020 IEEE Conference on Virtual Reality and 3D User Interfaces Abstracts and Workshops (VRW)* (2020), IEEE, pp. 838–839. 2
- [Aur91] AURENHAMMER F.: Voronoi diagrams—a survey of a fundamental geometric data structure. *ACM Computing Surveys (CSUR)* 23, 3 (1991), 345–405. 3
- [BSW*13] BOURNE R. R., STEVENS G. A., WHITE R. A., SMITH J. L., FLAXMAN S. R., PRICE H., JONAS J. B., KEEFFE J., LEASHER J., NAIDOO K., ET AL.: Causes of vision loss worldwide, 1990–2010: a systematic analysis. *The lancet global health* 1, 6 (2013), e339–e349. 2
- [CBH*11] CALABRESE A., BERNARD J.-B., HOFFART L., FAURE G., BAROUCH F., CONRATH J., CASTET E.: Wet versus dry age-related macular degeneration in patients with central field loss: different effects on maximum reading speed. *Investigative ophthalmology & visual science* 52, 5 (2011), 2417–2424. 4
- [DBP*15] DUSTLER M., BAKIC P., PETERSSON H., TIMBERG P., TINGBERG A., ZACKRISSON S.: Application of the fractal perlin noise algorithm for the generation of simulated breast tissue. In *Medical Imaging 2015: Physics of Medical Imaging* (2015), vol. 9412, International Society for Optics and Photonics, p. 94123E. 2
- [Dop18] DOPPIOSLASH C.: How shader development works. In *Physically Based Shader Development for Unity 2017*. Springer, 2018, pp. 3–16. 4
- [EMP*03] EBERT D. S., MUSGRAVE F. K., PEACHEY D., PERLIN K., WORLEY S.: *Texturing & modeling: a procedural approach*. Morgan Kaufmann, 2003. 3
- [FR99] FINE E. M., RUBIN G. S.: The effects of simulated cataract on reading with normal vision and simulated central scotoma. *Vision Research* 39, 25 (1999), 4274–4285. 1
- [HSSG12] HUBER P., SABER A., SCHNELLMANN Y., GOLD G.: Apprentissage de l'évaluation fonctionnelle par les étudiants en médecine: et si on simulait? *Revue médicale suisse* 8, 361 (2012), 2123–2127. 1
- [HZH*14] HU C. X., ZANGALLI C., HSIEH M., GUPTA L., WILLIAMS A. L., RICHMAN J., SPAETH G. L.: What do patients with glaucoma see? visual symptoms reported by patients with glaucoma. *The American journal of the medical sciences* 348, 5 (2014), 403–409. 3
- [JAR06] JIN B., AI Z., RASMUSSEN M.: Simulation of eye disease in virtual reality. In *2005 IEEE engineering in medicine and biology 27th annual conference* (2006), IEEE, pp. 5128–5131. 2
- [JBD*19] JAKES D., BURRAGE K., DROVANDI C. C., BURRAGE P., BUENO-OROVIO A., DOS SANTOS R. W., RODRIGUEZ B., LAWSON B. A.: Perlin noise generation of physiologically realistic patterns of fibrosis. *BioRxiv* (2019), 668848. 2
- [JMM08] JAGER R. D., MIELER W. F., MILLER J. W.: Age-related macular degeneration. *New England Journal of Medicine* 358, 24 (2008), 2606–2617. 2
- [JO18] JONES P. R., OMETTO G.: Degraded reality: Using vr/ar to simulate visual impairments. In *2018 IEEE Workshop on Augmented and Virtual Realities for Good (VAR4Good)* (2018), IEEE, pp. 1–4. 2
- [KBS*18] KRÖSL K., BAUER D., SCHWÄRZLER M., FUCHS H., SUTER G., WIMMER M.: A vr-based user study on the effects of vision impairments on recognition distances of escape-route signs in buildings. *The Visual Computer* 34, 6-8 (2018), 911–923. 2
- [KEL*20] KRÖSL K., ELVEZIO C., LUIDOLT L. R., HÜRBE M., KARST S., FEINER S., WIMMER M.: Cataract: Simulating cataracts in augmented reality. In *2020 IEEE International Symposium on Mixed and Augmented Reality (ISMAR)*. IEEE (2020). 2
- [KEW*19] KRÖSL K., ELVEZIO C., WIMMER M., HÜRBE M., FEINER S., KARST S.: Icthroughvr: Illuminating cataracts through virtual reality. In *2019 IEEE Conference on Virtual Reality and 3D User Interfaces (VR)* (2019), IEEE, pp. 655–663. 2, 3
- [KTH*09] KAMEDA T., TANABE T., HANGAI M., OJIMA T., AIKAWA H., YOSHIMURA N.: Fixation behavior in advanced stage glaucoma assessed by the microperimeter mp-1. *Japanese journal of ophthalmology* 53, 6 (2009), 580–587. 4
- [LBCM11] LEWIS J., BROWN D., CRANTON W., MASON R.: Simulating visual impairments using the unreal engine 3 game engine. In *2011 IEEE 1st International Conference on Serious Games and Applications for Health (SeGAH)* (2011), IEEE, pp. 1–8. 2
- [LDG*17] LAVALLIERE M., D'AMBROSIO L., GENNIS A., BURSTEIN A., GODFREY K. M., WAERSTAD H., PULEO R. M., LAUENROTH A., COUGHLIN J. F.: Walking a mile in another's shoes: The impact of wearing an age suit. *Gerontology & geriatrics education* 38, 2 (2017), 171–187. 1
- [LLC*10] LAGAE A., LEFEBVRE S., COOK R., DEROSE T., DRETAKIS G., EBERT D. S., LEWIS J. P., PERLIN K., ZWICKER M.: State of the art in procedural noise functions. *EG 2010-State of the Art Reports* (2010). 3
- [LRL*89] LEGGE G. E., ROSS J. A., LUEBKER A., LAMAY J. M., ET AL.: Psychophysics of reading. viii. the minnesota low-vision reading test. *Optom Vis Sci* 66, 12 (1989), 843–853. 4
- [MLC*20] MODJTAHEDI B. S., LUONG T. Q., CHIU S., VAN ZYL T., LIN J. C., FONG D. S.: Treatment course of patients with exudative age-related macular degeneration using ocular hypotensives. *Clinical Ophthalmology (Auckland, NZ)* 14 (2020), 187. 4
- [MV16] MIDENA E., VUJOSEVIC S.: Metamorphopsia: an overlooked visual symptom. *Ophthalmic research* 55, 1 (2016), 26–36. 3, 4
- [NFLS05] NAZEMI P. P., FINK W., LIM J. I., SADUN A. A.: Scotomas of age-related macular degeneration detected and characterized by means of a novel three-dimensional computer-automated visual field test. *Retina* 25, 4 (2005), 446–453. 3
- [O'S91] O'SHEA R. P.: Thumb's rule tested: visual angle of thumb's width is about 2 deg. *Perception* 20, 3 (1991), 415–418. 2
- [PFW*98] POINOOSAWMY D., FONTANA L., WU J. X., BUNCE C. V., HITCHINGS R. A.: Frequency of asymmetric visual field defects in normal-tension and high-tension glaucoma. *Ophthalmology* 105, 6 (1998), 988–991. 2
- [PSK*16] PATNEY A., SALVI M., KIM J., KAPLANYAN A., WYMAN C., BENTY N., LUEBKE D., LEFOHN A.: Towards foveated rendering for gaze-tracked virtual reality. *ACM Transactions on Graphics (TOG)* 35, 6 (2016), 179. 2
- [Qui99] QUILLEN D. A.: Common causes of vision loss in elderly patients. *American family physician* 60, 1 (1999), 99–108. 2, 3
- [SA05] SUNNESS J. S., APPLGATE C. A.: Long-term follow-up of fixation patterns in eyes with central scotomas from geographic atrophy that is associated with age-related macular degeneration. *American journal of ophthalmology* 140, 6 (2005), 1085–1093. 4
- [SES18] STOCK S., ERLER C., STORK W.: Realistic simulation of progressive vision diseases in virtual reality. In *Proceedings of the 24th ACM Symposium on Virtual Reality Software and Technology* (2018), pp. 1–2. 2
- [SIGK*16] SWAFFORD N. T., IGLESIAS-GUITIAN J. A., KONIARIS C., MOON B., COSKER D., MITCHELL K.: User, metric, and computational evaluation of foveated rendering methods. In *Proceedings of the ACM Symposium on Applied Perception* (2016), pp. 7–14. 2

- [TEBC18] TAYLOR D. J., EDWARDS L. A., BINNS A. M., CRABB D. P.: Seeing it differently: self-reported description of vision loss in dry age-related macular degeneration. *Ophthalmic and Physiological Optics* 38, 1 (2018), 98–105. [3](#)
- [TMGS94] TOLENTINO M. J., MILLER S., GAUDIO A. R., SANDBERG M. A.: Visual field deficits in early age-related macular degeneration. *Vision research* 34, 3 (1994), 409–413. [3](#)
- [VAS08] VINNIKOV M., ALLISON R. S., SWIERAD D.: Real-time simulation of visual defects with gaze-contingent display. In *Proceedings of the 2008 symposium on Eye tracking research & applications* (2008), pp. 127–130. [2](#)
- [VCH16] VÄYRYNEN J., COLLEY A., HÄKKILÄ J.: Head mounted display design tool for simulating visual disabilities. In *Proceedings of the 15th International Conference on Mobile and Ubiquitous Multimedia* (2016), pp. 69–73. [2](#)
- [WAM14] WEINREB R. N., AUNG T., MEDEIROS F. A.: The pathophysiology and treatment of glaucoma: a review. *Jama* 311, 18 (2014), 1901–1911. [3](#)
- [WSL*14] WONG W. L., SU X., LI X., CHEUNG C. M. G., KLEIN R., CHENG C.-Y., WONG T. Y.: Global prevalence of age-related macular degeneration and disease burden projection for 2020 and 2040: a systematic review and meta-analysis. *The Lancet Global Health* 2, 2 (2014), e106–e116. [2](#)
- [XHH10] XUEMEI L., HUAN L., HUI Y.: Generation of organ texture with perlin noise. In *2010 International Conference on E-Health Networking Digital Ecosystems and Technologies (EDT)* (2010), vol. 1, IEEE, pp. 150–152. [2](#)
- [ZL18] ZAVLANOU C., LANITIS A.: Product packaging evaluation through the eyes of elderly people: personas vs. aging suit vs. virtual reality aging simulation. In *International Conference on Human Systems Engineering and Design: Future Trends and Applications* (2018), Springer, pp. 567–572. [2](#)